ACS Macro Letters

pubs.acs.org/macroletters Letter

Surface-Grafted Polymeric Ionic Liquids with Tunable Morphology via *In/Ex Situ* Cross-linking Methods

Serkan Demirci,* Selin Kinali-Demirci, and Brett VanVeller*

Cite This: *ACS Macro Lett.* 2020, 9, 1806−1811 Read Online

ACCESS | Metrics & More | Article Recommendations | Supporting Information

ABSTRACT: Surface-grafted poly(ionic liquid) (PIL) films were prepared by both *in* and *ex situ* cross-linking methods with reversible addition−fragmentation chain transfer (RAFT) polymerization. Cross-linked brushes are more stable than linear brushes without sacrificing the surface functionality and, therefore, have increased potential for applications in biomedicine and materials chemistry. The two methods, *in situ* via a bifunctional cross-linker and *ex situ* via thermal cross-linking, were systematically compared on silicon-wafer substrates. Films obtained through *in situ* cross-linking were superior to films derived from our *ex situ* cross-linking technique with respect to responsive behavior and controlling the formation of polymer brushes on the surface. Alternatively, more stable layers were obtained by the *ex situ* cross-linking method using a cross-linker based on Meldrum's acid, where the film structure could be changed from a brush to collapsed film morphologies with an increasing cross-linker ratio.

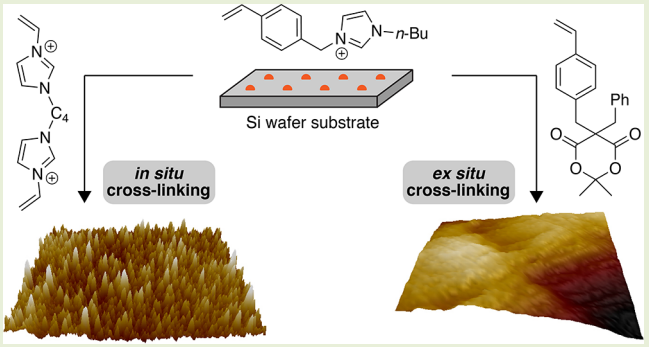

The development of new surface technologies demands precise control of the interface properties such as adhesion, friction, environmental response, and biocompatibility. The diversity of polymers and their functional groups makes them a powerful tool to achieve control of the properties of surfaces. Polymer brushes, in particular, have received increasing attention to tune surface characteristics.[1−4]

A polymer brush architecture is created by the attachment of one end of a macromolecule to a surface or interface, which creates a surface-bound film with properties that can be controlled by the identity of the polymer.[5,6] The stability of a polymer film displayed on a surface is of vital importance to a broad spectrum of applications including coating, adhesion, and biotechnology,[7] where harsh environments can result in the slow destruction of the brush film as polymer chains are broken or torn away from the substrate.[8] Numerous strategies have been proposed to stabilize polymer films including: polymer cross-linking, block copolymers, the addition of nanoparticles or other components to the film, and grafted polymer brushes.[9−11] Cross-linked polymer brushes, often called polymer brush gels, display many of the characteristics of polymer brushes, but the cross-links allow for further tuning of the swelling and mechanical characteristics of the film. Surface-grafted polymer-gels can be prepared using two different methods termed *in situ* and *ex situ* (Scheme 1).[10−12] For the *in situ* method, cross-linking of the polymer chains takes place simultaneously with chain-growth polymerization from the surface. Alternatively, for the *ex situ* method, polymer gels are prepared by cross-linking the chains in a postmodification step that follows polymerization from the surface.[12,13]

Scheme 1. Preparation of Cross-linked Polymer via *In Situ* and *Ex Situ* Cross-linking Methods

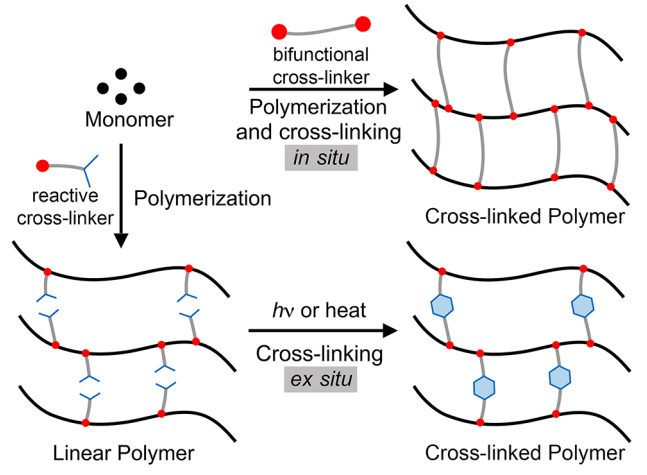

Received: September 2, 2020
Accepted: November 23, 2020
Published: November 25, 2020

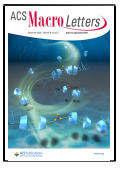

https://dx.doi.org/10.1021/acsmacrolett.0c00632
ACS Macro Lett. 2020, 9, 1806−1811

We describe the development of surface-grafted and cross-linked poly(ionic liquid) films to address challenges in surface stability without sacrificing surface functionality. Polymeric ionic liquids, also called poly(ionic liquid)s (PILs), are polymers prepared by the polymerization of ionic liquid monomers.[14−16] PILs are a relatively new class of functional polymeric materials, combining the unique properties of molecular ionic liquids with the processability of polymers.[17,18] Recently, interest in PILs has increased due to their excellent mechanical and electrochemical properties such as high thermal stability, biocompatibility, and inherent conductivity.[18−20] Accordingly, PILs have been investigated for applications in catalytic membranes, ionic conductive materials, solid state polyelectrolytes, catalysts, biosensors, matrices for enzyme immobilization, CO_2 absorbing resins, and microwave absorbing materials.[18,21−24] Yet, studies dealing with PIL brush architectures are more limited in the literature.[24−28]

We have prepared highly stable and responsive PIL layers from surface-grafted and cross-linked PIL films by employing *in* and *ex situ* methods through reversible addition−fragmentation chain transfer (RAFT) polymerization. The PIL layers were characterized by XPS, AFM, ellipsometry, and static water contact angle measurements. Surface-grafted and covalently cross-linked PILs were shown to be versatile and chemically stable films with highly tunable properties at a nearly constant chemical composition. We believe that surface functionalization with this class of brush layer could be a promising approach for independently tailoring the chemical and mechanical properties of a variety of materials.

For the sake of clarity, PIL layers obtained with different methods are named **Ia−c**, **Ea−c**, and **ECa−c**, indicating PIL films prepared via the *in situ* cross-linking method (**I**) and the *ex situ* cross-linking method before (**E**) and after cross-linking (**EC**) with variable cross-linker ratios (**a**, **b**, and **c** for 1, 5, and 10 mol % of monomer, respectively).

All polymer films were fabricated through immobilization of RAFT agent on amine-terminated silicon wafers (Scheme 2).[25] Polymerizations were carried out using 2,2′-azobis(2,4-dimethylvaleronitrile) (ABVN) as the initiator in a glass reactor under the rigorous exclusion of oxygen (three cycles of freeze−pump−thaw).

To obtain cross-linked films via the *in situ* method (**Ia−c**, Scheme 2), surface-initiated RAFT polymerization was undertaken using the ionic liquid monomer 1-vinylbenzyl-3-butylimidazolium bromide (VBIC) and bifunctional cross-linker 1,4-di(3-vinylimidazolium)butane dibromide (DVIMBr) added at molar ratios relative to the monomer of **a**, **b**, and **c** described above.

For the *ex situ* cross-linking method (**Ea−c**, Scheme 2), surface-initiated RAFT polymerization was carried out using the ionic liquid monomer of VBIC as a monomer and a masked cross-linker 5-benzyl-2,2-dimethyl-5-(4-vinylbenzyl)-[1,3]dioxane-4,6-dione based on Meldrum's acid (Meldrum's cross-linker).[29] The Meldrum's cross-linker was added at the molar ratios relative to the monomer of **a**, **b**, and **c** described above. Subsequent thermolysis of substrates **Ea−c** at 250 °C for 10 min converted the masked Meldrum's cross-linker to a highly reactive ketene for simultaneous cross-linking of polymer chains with the possibility for reaction with free amine groups on the silicon substrate (**ECa−c**).

XPS measurements were used to monitor the surface chemical composition change of each reaction step. A full description and interpretation of the XPS results can be found in Figure S2 and Table S1, where a brief description of key results follows. The identity of the amine-modified silicon wafers was confirmed by the appearance of an N 1s signal at 400 eV. Similarly, the attachment of the chain transfer agent (CTA) was confirmed by the appearance of an S 2p signal at 100 eV.[30,31] The XPS spectra of the amine and CTA modified silicon wafers include a weak Si signal originating from the silicon substrate, whereas no Si signal was observed in the case of the **Ia−c**, **Ea−c**, and **ECa−c**. For **Ia**, obtained via the *in situ* method, peak components attributed to the C−N bonds and the C═C/C−C bonds can be identified, whereas substrates obtained via the *ex situ* method, **Ea−c**, displayed additional peaks assigned to O−C−O and O−C═O bonds as anticipated. After thermolysis, XPS results clearly show the disappearance of O−C−O and O−C═O peaks and the appearance of a C═O peak due to the ketene dimerization provided by the cross-linking (**ECa**), signifying that polymer chains were cross-linked in the structure.

AFM experiments were performed to study the surface morphology of PIL layers in more detail (Figure 1 for representative examples and Figure S3). For **Ia−c**, the film morphologies appeared as rod-like structures heterogeneously distributed over the entire substrate area, where the root-mean-square (RMS) roughness of **Ia**, **Ib**, and **Ic** PIL brush gels was 6.000, 7.167, and 7.732 nm, respectively. We attribute the increase in surface roughness to spatial variation caused by the increasing cross-linking density, which leads to the clustering of the growing chains. This interpretation is supported by the observation that the *in situ* brush layer with the lowest percentage of cross-linker (1%, **Ia**) showed a comparable RMS value with the uncross-linked *ex situ* brush layers **Ea−c**. In addition, the noticeably higher roughness of **Ib** and **Ic** suggests a more rigid structure with a higher cross-linker ratio and thus indicates higher free volume within those cross-linked brushes.

Scheme 2. Schematic Illustration of the Preparation of PIL Brushes and Brush Gels and the Chemical Structure of RAFT Agent, IL Monomer, and Cross-linkers

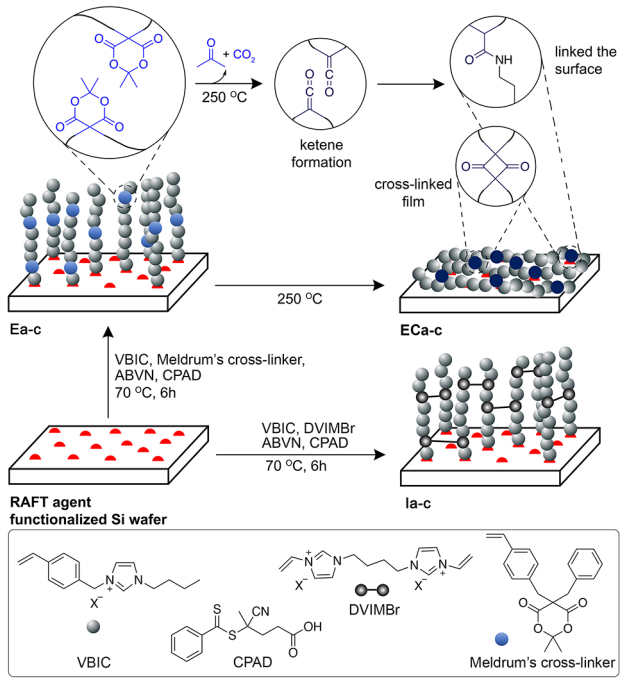

https://dx.doi.org/10.1021/acsmacrolett.0c00632
ACS Macro Lett. 2020, 9, 1806−1811

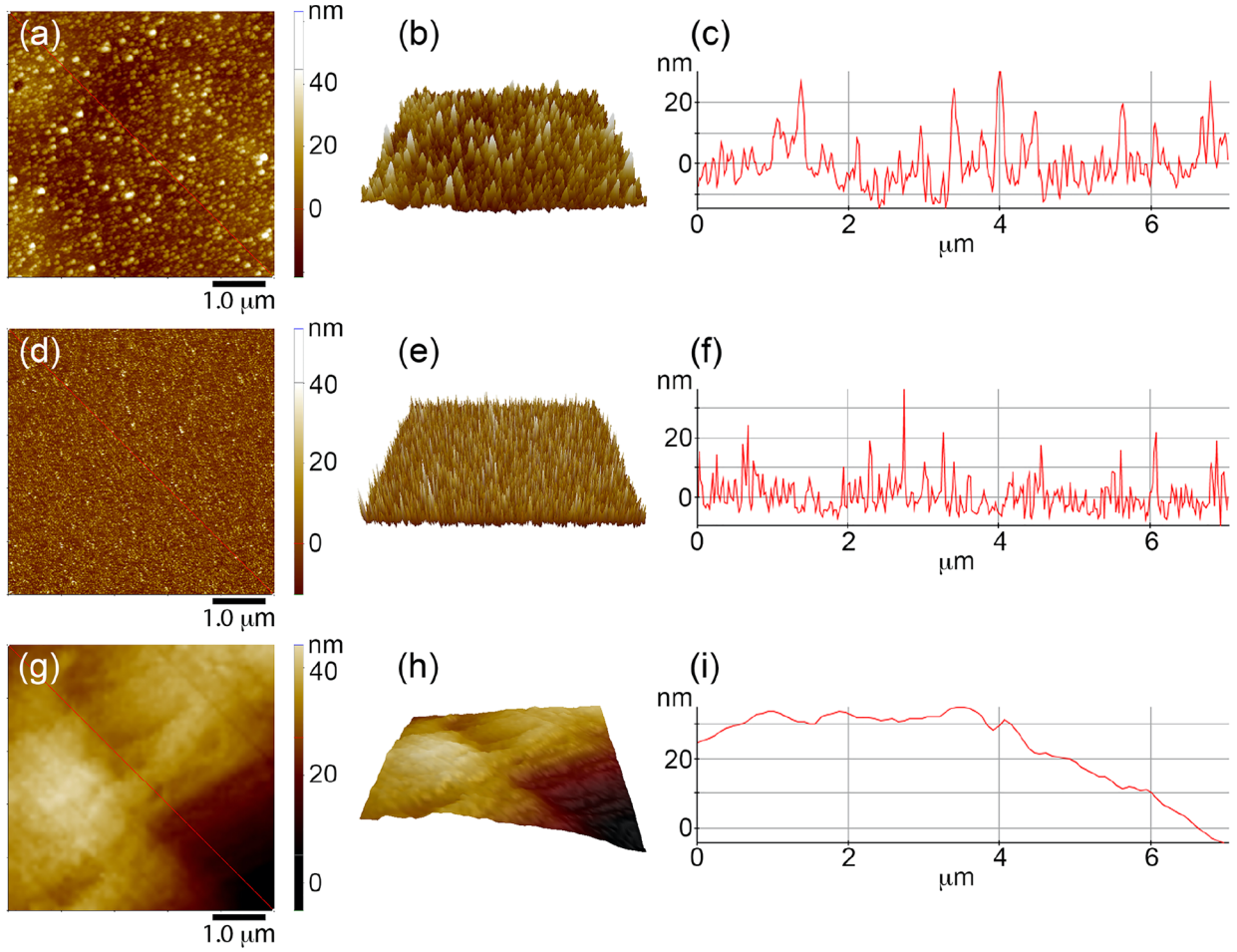

Figure 1. 2D and 3D surface topography and cross-section profiles at red lines of 5 μm images of **Ia** (a–c), **Ea** (d–f), and **ECa** (g–i) PIL coatings on Si wafers prepared via *in/ex situ* methods.

Finally, the ellipsometric thicknesses of the PIL brush gels of 41 ± 8, 38 ± 5 and 47 ± 6 nm for **Ia**, **Ib**, and **Ic**, respectively, were similar within error.

Similar to results from our previous study,[30−32] uncross-linked PIL brushes (**Ea**–**c**) prepared by RAFT polymerization exhibited needle-like structures, where the roughness indicated by the RMS values was 4.221, 4.803, and 5.770 nm. The ellipsometric thicknesses of the PIL brushes were also similar to 34 ± 5, 39 ± 6, and 33 ± 3 nm for **Ea**, **Eb**, and **Ec**, respectively.

For uncross-linked **Ea**–**c**, grafting parameters, including grafting density (σ, chains/nm^2), the average distance between grafting sites (D, nm) and the radius of gyration (R_g, nm) was calculated from the dry ellipsometric thicknesses using eqs 1–3 given in the Supporting Information. The grafting density of the **Ea**–**c** was estimated to be 0.72, 0.78, and 0.65 chains/nm^2 for **Ea**, **Eb**, and **Ec**, respectively (Table S2). A comparison of the average distance between the grafting points with twice the radius of gyration of the PIL chain resulted in a ratio of 0.24 (less than 1.0), which means that the grafted chains are indeed in a stretched and brush-like conformation.

Significant topographical changes in surface roughness and ellipsometric thickness appeared in the films prepared via the *ex situ* cross-linking method (**ECa**–**c**, Figure 1g). We hypothesize that, because of the steric hindrance of the RAFT agent, there is a potential for unreacted amine groups to persist on the surface after functionalization with RAFT agent.[30,33] Following ketene generation to cross-link the film (Scheme 2, ketene dimerization), the reactive ketene units can likely also react with free amine groups on the surface to produce contracted **EC** films (Figures 1g–i and S3). For example, the linear brush **Ea** contracted from 34 ± 5 to 12 ± 3 nm (ellipsometric thicknesses) upon cross-linking, and AFM analysis revealed a far smoother layer with an RMS roughness of 1.011 nm. The films (**ECb**-**c**) appear as macroscopically homogeneous thin films with an increasing cross-linker ratio from 1% to 5% and 10%. However, the formation of bubbles (CO_2) during the thermolysis and a corresponding increase in film roughness were observed. RMS roughness of the film increased from 1.873 nm to 2.371 and 4.956 nm due to the development of bumps within the layer. The ellipsometric thicknesses of **ECb** and **ECc** were measured to be 15 ± 6 and 14 ± 7 nm, respectively.

On the basis of these observations, we may conclude that *in/ex situ* approaches to surface-grafted and cross-linked PILs can tailor the surface properties from an extended homogeneous brush layer to a collapsed morphology.

Finally, the wettability of the PIL films can be manipulated from hydrophilic to hydrophobic through anion exchange.[25,34,35] To investigate these effects on the different morphologies described here, the more hydrophilic PIL surfaces containing Br as the counteranion were converted to comparatively hydrophobic surfaces through immersion and anion exchange in a solution of lithium bis(trifluoromethane)-

https://dx.doi.org/10.1021/acsmacrolett.0c00632
ACS Macro Lett. 2020, 9, 1806−1811

sulfonimide (LiTSFI). The wettability characteristics of each surface were then probed using water-droplet contact angle measurements (Figure 2 and Table S3).

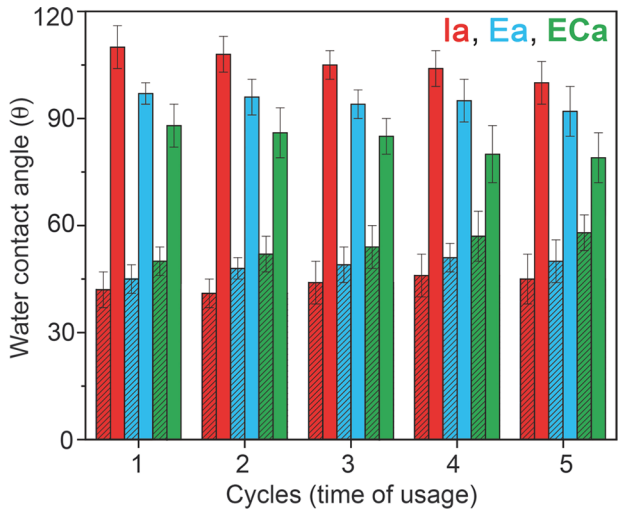

Figure 2. Water contact angles of Br (patterned) and TFSI films of **Ia**, **Ea**, and **ECa** in repeated cycles.

As anticipated, films containing Br anions displayed comparatively hydrophilic properties with contact angles up to 39° and around 42° for **I**-Br and **E**-Br, respectively. After anion exchange with TSFI, contact angles increased to ∼100° and the films exhibited more hydrophobic properties. The **EC** films prepared by the *ex situ* method displayed similar but more modest changes in their hydrophilic and hydrophilic character (Figure 2 and Table S3).

The topographical heterogeneity of each film was further probed through contact angle hysteresis, in which the surface is tilted until the droplet begins to slide. At this moment, the advancing angle (θ_a) of the droplet defines the maximum contact angle of the surface, while the receding angle (θ_r) defines the minimum contact angle of the surface (where hysteresis is defined by $\Delta\theta = \theta_a - \theta_r$, Table S3). In general, cross-linked surfaces prepared by the *in situ* method (**Ia**−**c**) displayed higher hysteresis than the linear brush films **Ea**−**c**. Accordingly, the *ex situ* cross-linked films **ECa**−**c** displayed even lower values of hysteresis pointing to less heterogeneity with respect to roughness and wetting behavior overall. These results align with observations by AFM described above and further support our conclusions that the different *in*/*ex situ* approaches can tailor different surface morphologies.

The reversible wetting behavior of the **Ia**−**c**, **Ea**−**c**, and **ECa**−**c** films was investigated by cycling the anion-exchange procedure 5 times (Figure 2) and measuring the water-droplet contact angle. The result of each cycle revealed that the surfaces can be reversibly changed between hydrophilic (Br) and hydrophobic (TFSI) properties within error.

To examine the **Ia**−**c**, **Ea**−**c**, and **ECa**−**c** films' durability, PIL modified surfaces were incubated in the rotary flow system for 72 h at 37 °C, and the dry thickness of the PIL layers was measured by ellipsometry. The dry thickness of **I** and **EC** hardly changed because of the cross-linked structure (Figure S4). In contrast, the thickness of **Ea**−**c** dramatically decreased upon incubation. These results indicate that the cross-linked polymer brushes are highly durable compared to the linear polymer brushes.

The swelling properties of the PIL-coated surfaces was examined by determining the swelling ratios, which are defined as the ratio of the thickness of the swollen (h_s) and dry (h_d) films. The swelling ratio as a function of the cross-linker ratio is shown in Figure 3 for **Ia**−**c**, **Ea**−**c**, and **ECa**−**c**. As expected,

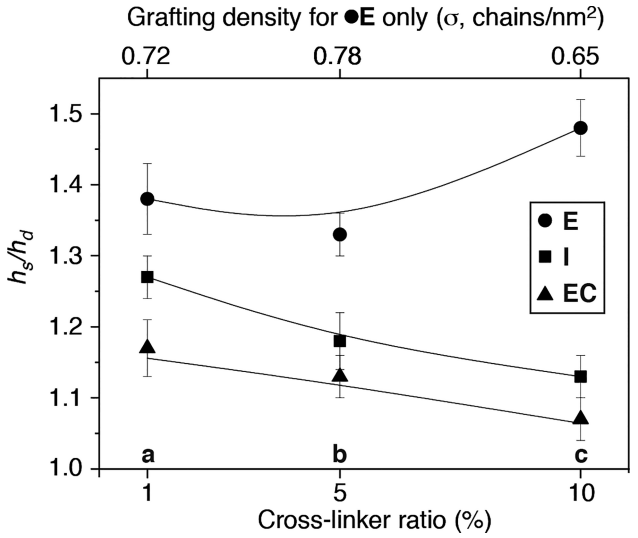

Figure 3. Swelling ratio h_s/h_d of **Ia**−**c**, **Ea**−**c**, **ECa**−**c** layers as a function of cross-linker ratio. The swelling ratio for **Ea**−**c** brushes corresponding to different grafting densities.

the swelling ratio for both **Ia**−**c** and **ECa**−**c** decreased with increasing cross-linker ratio. Notably, the collapsed PIL layers, **ECa**−**c**, showed the lowest swelling ratios overall.

The swelling ratio trend for **Ea**−**c** was different because those films had not yet been cross-linked. In this case, the graft density is a more telling metric of the swelling behavior. In accordance with literature precedent,[36−38] higher ratios of swelling (h_s/h_d) were observed for **Ec** brushes with lower grafting density.

In summary, we have designed and synthesized novel PIL brushes and brush gels through surface-initiated RAFT polymerization. Two distinct approaches involving both *in situ* and *ex situ* methods were exploited to realize films with distinct surface characteristics depending on the method of fabrication. The observed results demonstrate that *in*/*ex situ* methods could be utilized to tailor surface-grafted and cross-linked PILs from a stretched homogeneous brush-like layer to a collapsed film. The two methods may be used in combination to realize surfaces with intermediate properties. These cross-linked PIL films provide the potential for surface stability without sacrificing the functional behavior of PILs.

■ ASSOCIATED CONTENT

Supporting Information

The Supporting Information is available free of charge at https://pubs.acs.org/doi/10.1021/acsmacrolett.0c00632.

Synthetic procedure and characterization of small molecules and polymers, XPS and AFM characterization of surfaces, grafting parameters of **Ea**−**c**, atomic concentration, water contact angle, and dry thickness of PIL layers (PDF)

https://dx.doi.org/10.1021/acsmacrolett.0c00632
ACS Macro Lett. 2020, 9, 1806−1811

AUTHOR INFORMATION

Corresponding Authors

Serkan Demirci − *Department of Chemistry, Iowa State University, Ames, Iowa 50011, United States; Department of Chemistry, Amasya University, Ipekkoy, Amasya 05100, Turkey;* orcid.org/0000-0002-4753-2069; Email: srkndemirci@gmail.com, sdemirci@amasya.edu.tr

Brett VanVeller − *Department of Chemistry, Iowa State University, Ames, Iowa 50011, United States;* orcid.org/0000-0002-3792-0308; Email: bvv@iastate.edu

Author

Selin Kinali-Demirci − *Department of Chemistry, Iowa State University, Ames, Iowa 50011, United States; Department of Chemistry, Amasya University, Ipekkoy, Amasya 05100, Turkey;* orcid.org/0000-0001-5363-9412

Complete contact information is available at: https://pubs.acs.org/10.1021/acsmacrolett.0c00632

Notes

The authors declare no competing financial interest.

ACKNOWLEDGMENTS

S.D. received financial support from TUBITAK-BIDEB 2219-International Postdoctoral Research Fellowship Programme for this study. B.V. acknowledges the National Science Foundation, Division of Chemistry (grant no. 1848261).

REFERENCES

(1) Senaratne, W.; Andruzzi, L.; Ober, C. K. Self-Assembled Monolayers and Polymer Brushes in Biotechnology: Current Applications and Future Perspectives. *Biomacromolecules* **2005**, *6*, 2427−2448.

(2) Yuksekdag, Y. N.; Gevrek, T. N.; Sanyal, A. Diels-Alder "Clickable" Polymer Brushes: A Versatile Catalyst-Free Conjugation Platform. *ACS Macro Lett.* **2017**, *6*, 415−420.

(3) Demirci, S.; Kinali-Demirci, S.; Jiang, S. A Switchable Polymer Brush System for Antifouling and Controlled Detection. *Chem. Commun.* **2017**, *53*, 3713−3716.

(4) Krishnamoorthy, M.; Hakobyan, S.; Ramstedt, M.; Gautrot, J. E. Surface-Initiated Polymer Brushes in the Biomedical Field: Applications in Membrane Science, Biosensing, Cell Culture, Regenerative Medicine and Antibacterial Coatings. *Chem. Rev.* **2014**, *114*, 10976−11026.

(5) Chen, W.-L.; Cordero, R.; Tran, H.; Ober, C. K. 50th Anniversary Perspective: Polymer Brushes: Novel Surfaces for Future Materials. *Macromolecules* **2017**, *50*, 4089−4113.

(6) Krishnamoorthy, M.; Hakobyan, S.; Ramstedt, M.; Gautrot, J. E. Surface-Initiated Polymer Brushes in the Biomedical Field: Applications in Membrane Science, Biosensing, Cell Culture, Regenerative Medicine and Antibacterial Coatings. *Chem. Rev.* **2014**, *114*, 10976−11026.

(7) Xia, B.; Dong, C.; Lu, Y.; Rong, M.; Lv, Y.-Z.; Shi, J. Preparation and Characterization of Chemically-Crosslinked Polyethyleneimine Films on Hydroxylated Surfaces for Stable Bactericidal Coatings. *Thin Solid Films* **2011**, *520*, 1120−1124.

(8) Hoffmann, M.; Lang, M.; Sommer, J.-U. Gelation Threshold of Cross-Linked Polymer Brushes. *Phys. Rev. E* **2011**, *83*, 021803.

(9) Demirci, S. Crosslinked-Polymer Brushes with Switchable Capture and Release Capabilities. *Polymers* **2018**, *10*, 956.

(10) Dehghani, E. S.; Spencer, N. D.; Ramakrishna, S. N.; Benetti, E. M. Cross-linking Polymer Brushes with Ethylene Glycol-Containing Segments: Influence on Physicochemical and Antifouling Properties. *Langmuir* **2016**, *32*, 10317−10327.

(11) Dehghani, E. S.; Aghion, S.; Anwand, W.; Consolatie, G.; Ferragut, R.; Panzarasa, G. Investigating the Structure of Crosslinked Polymer Brushes (Brush-Gels) by Means of Positron Annihilation Spectroscopy. *Eur. Polym. J.* **2018**, *99*, 415−421.

(12) Li, A.; Benetti, E. M.; Tranchida, D.; Clasohm, J. N.; Schönherr, H.; Spencer, D. N. Surface-Grafted, Covalently Cross-linked Hydrogel Brushes with Tunable Interfacial and Bulk Properties. *Macromolecules* **2011**, *44*, 5344−5351.

(13) Loveless, D. M.; Abu-Lail, N. I.; Kaholek, M.; Zauscher, S.; Craig, S. L. Reversibly Cross-linked Surface-grafted Polymer Brushes. *Angew. Chem., Int. Ed.* **2006**, *45*, 7812−7814.

(14) Yuan, J.; Antonietti, M. Poly(ionic liquid)s: Polymers Expanding Classical Property Profiles. *Polymer* **2011**, *52*, 1469−1482.

(15) Isik, M.; Gracia, R.; Kollnus, L. C.; Tome, L. C.; Marrucho, I. M.; Mecerreyes, D. Cholinium-based Poly(ionic liquid)s: Synthesis, Characterization, and Application as Biocompatible Ion Gels and Cellulose Coatings. *ACS Macro Lett.* **2013**, *2*, 975−979.

(16) Mecerreyes, D. Polymeric Ionic Liquids: Broadening the Properties and Applications of Polyelectrolytes. *Prog. Polym. Sci.* **2011**, *36*, 1629−1648.

(17) Devasurendra, A. M.; Zhang, C.; Young, J. A.; Tillekeratne, L. M. V.; Anderson, J. L.; Kirchhoff, J. R. Electropolymerized Pyrrole-Based Conductive Polymeric Ionic Liquids and Their Application for Solid-Phase Microextraction. *ACS Appl. Mater. Interfaces* **2017**, *9*, 24955−24963.

(18) Grygiel, K.; Lee, J.-S.; Sakaushi, K.; Antonietti, M.; Yuan, Y. Thiazolium Poly(ionic liquid)s: Synthesis and Application as Binder for Lithium-ion Batteries. *ACS Macro Lett.* **2015**, *4*, 1312−1316.

(19) Zhao, Q.; Dunlop, J. W. C.; Qiu, X.; Huang, F.; Zhang, Z.; Heyda, J.; Dzubiella, J.; Antonietti, M.; Yuan, J. An Instant Multi-responsive Porous Polymer Actuator Driven by Solvent Molecule Sorption. *Nat. Commun.* **2014**, *5*, 4293.

(20) Zhang, Q.; Zhang, S.; Deng, Y. Recent Advances in Ionic Liquid Catalysis. *Green Chem.* **2011**, *13*, 2619−2637.

(21) Zhang, W.; Yang, T.; Zhuang, X.; Guo, Z.; Jiao, K. An Ionic Liquid Supported CeO_2 Nanoshuttles-Carbon Nanotubes Composite as a Platform for Impedance DNA Hybridization Sensing. *Biosens. Bioelectron.* **2009**, *24*, 2417−2422.

(22) Ramdin, M.; de Loos, T. W.; Vlugt, T. J. H. State-of-the-Art of CO_2 Capture with Ionic Liquids. *Ind. Eng. Chem. Res.* **2012**, *51*, 8149−8177.

(23) Tauber, K.; Dani, A.; Yuan, J. Covalent Cross-Linking of Porous Poly(ionic liquid) Membrane via a Triazine Network. *ACS Macro Lett.* **2017**, *6*, 1−5.

(24) Dong, Y.-S.; Xiong, X.-H.; Lu, X.-W.; Wu, Z.-Q.; Chen, H. Antibacterial Surfaces Based on Poly(cationic liquid) Brushes: Switchability Between Killing and Releasing via Anion Counterion Switching. *J. Mater. Chem. B* **2016**, *4*, 6111.

(25) Demirci, S.; Kinali-Demirci, S.; VanVeller, B. Controlled Supramolecular Complexation of Cyclodextrin-Functionalized Polymeric Ionic Liquid Brushes. *ACS Appl. Polym. Mater.* **2020**, *2*, 751−757.

(26) He, X.; Yang, W.; Pei, X. Preparation, Characterization, and Tunable Wettability of Poly(ionic liquid) Brushes via Surface-Initiated Atom Transfer Radical Polymerization. *Macromolecules* **2008**, *41*, 4615−4621.

(27) Li, Z.; He, G.; Li, Z.; Zhang, Y.; Zhao, J.; Xu, M.; Xu, S.; Jiang, Z. Enhancing the Hydroxide Conductivity of Imidazolium-Functionalized Polysulfone by Incorporating Organic Microsphere with Ionic Brushes. *J. Membr. Sci.* **2018**, *554*, 6−15.

(28) Yu, L.; Zhang, Y.; Wang, Y.; Zhang, H.; Liu, J. High flux, Positively Charged Loose Nanofiltration Membrane by Blending with Poly(ionic liquid) Brushes Grafted Silica Spheres. *J. Hazard. Mater.* **2015**, *287*, 373−383.

(29) Leibfarth, F. A.; Kang, M.; Ham, M.; Kim, J.; Campos, L. M.; Gupta, N.; Moon, B.; Hawker, C. J. A Facile Route to Ketene-Functionalized Polymers for General Materials Applications. *Nat. Chem.* **2010**, *2*, 207−212.

(30) Gurbuz, N.; Demirci, S.; Yavuz, S.; Caykara, T. Synthesis of Cationic *N*-[3-(Dimethylamino)propyl]methacrylamide Brushes on

Silicon Wafer via Surface-Initiated RAFT Polymerization. *J. Polym. Sci., Part A: Polym. Chem.* **2011**, *49*, 423−431.
(31) Demirci, S.; Kinali-Demirci, S.; Caykara, T. Novel pH-Responsive Mixed-Charge Copolymer Brushes Based on Carboxylic Acid and Quaternary Amine Monomers. *J. Polym. Sci., Part A: Polym. Chem.* **2013**, *51*, 1612−1619.
(32) Demirci, S.; Caykara, T. Controlled Grafting of Cationic Poly[(*ar*-vinylbenzyl)trimethyl ammonium chloride] on Hydrogen-Terminated Silicon Substrate by Surface-Initiated RAFT Polymerization. *React. Funct. Polym.* **2012**, *72*, 588−595.
(33) Demirci, S.; Caykara, T. RAFT-mediated Synthesis of Cationic Poly[(ar-vinylbenzyl)trimethyl ammonium chloride] Brushes for Quantitative DNA Immobilization. *Mater. Sci. Eng., C* **2013**, *33*, 111−120.
(34) Guo, J.; Xu, Q.; Zheng, Z.; Zhou, S.; Mao, H.; Wang, B.; Yan, F. Intrinsically Antibacterial Poly(ionic liquid) Membranes: The Synergistic Effect of Anions. *ACS Macro Lett.* **2015**, *4*, 1094−1098.
(35) Zhang, S. Y.; Zhuang, Q.; Zhang, M.; Wang, H.; Gao, Z.; Sun, J. K.; Yuan, J. Poly(ionic liquid) Composites. *Chem. Soc. Rev.* **2020**, *49*, 1726−1755.
(36) Malham, I. B.; Bureau, L. Density Effect on Collapse, Compression and Adhesion of Thermoresponsive Polymer Brushes. *Langmuir* **2010**, *26*, 4762−4768.
(37) Horst, R. J.; Perez, M. B.; Cohen, R.; Cirelli, M.; Robles, S. D.; Elshof, M. G.; Andreski, A.; Hempenius, M. A.; Benes, N. E.; Damen, C.; Beer, S. Swelling of Poly(methyl acrylate) Brushes in Acetone Vapor. *Langmuir* **2020**, *36*, 12053−12060.
(38) Biesalski, M.; Rühe, J. Scaling Laws for Swelling of Neutral and Charged Polymer Brushes in Good Solvents. *Macromolecules* **2002**, *35*, 499−507.

https://dx.doi.org/10.1021/acsmacrolett.0c00632
ACS Macro Lett. 2020, 9, 1806−1811